Development of relative positioning algorithms for agricultural drone swarms in GPS-challenged environments

Maksym Ogurtsov[1,*,†], Vyacheslav Korolyov[1,†], Oleksandr Khodzinsky[1,†] and Oleh Rybalchenko[1,†]

[1] *V.M. Glushkov Institute of Cybernetics of the National Academy of Sciences of Ukraine, Ac. Hlushkova str. 40, building 1, apt. 801 03187 Kyiv, Ukraine*

Abstract

In recent years, agricultural drones have significantly increased use for tasks such as field irrigation, pest detection, and crop health monitoring. To improve operational efficiency and speed across extensive agricultural regions, the deployment of drone swarms is becoming increasingly prevalent. However, in remote regions where Global Positioning System (GPS) signals may be inaccurate or unavailable and real-time kinematic services are expensive, the need arises for effective methods to determine the precise relative positions of drones within a swarm.

The purpose of this work is to develop relative positioning algorithms for agricultural drone swarms in GPS-challenged environments. These algorithms should enable the determination of the relative positions of drones and the overall configuration of the swarm even in the complete absence of GPS signals.

As a result of this study, an algorithm for determining the relative position of swarm elements in the absence of global positioning signals and the corresponding mathematical apparatus was developed. It takes into account possible inaccuracy of distance measurement.

Various configurations of possible relative positions of swarm elements, their impact on determining the relative position, and possible solutions to problems in case of an unsuccessful initial arrangement were analyzed. The obtained results were successfully confirmed by practical calculations.

Keywords

UAV, drone, swarm, swarm control, local positioning, GPS, geometry

1. Introduction

In recent years, agricultural drones have significantly increased use for tasks such as field irrigation, pest detection, and crop health monitoring [1]. To enhance the efficiency and speed of operations over large agricultural areas, drone swarms are increasingly being used [2]. However, in remote regions where Global Positioning System (GPS) signals may be inaccurate or unavailable, the need arises for effective methods to determine the precise relative positions of drones within a swarm to prevent collisions and ensure high-precision task execution [3].

Proposed solutions that are used nowadays typically rely on expensive networks of fixed stations (anchors) with verified positions [4].

Information Technology and Implementation (IT&I-2024), November 20-21, 2024, Kyiv, Ukraine

* Corresponding author.

† These authors contributed equally.

maksymogurtsov@gmail.com (M. Ogurtsov); korolev.academ@gmail.com (V. Korolyov); okhodz@gmail.com (O. Khodzinsky); rv.oleg.ua@gmail.com (O. Rybalchenko)

0000-0002-6167-5111 (M. Ogurtsov); 0000-0003-1143-5846 (V. Korolyov); 0000-0003-4574-3628 (O. Khodzinsky); 0000-0002-5716-030X (O. Rybalchenko)

2. Goal

The purpose of this work is to develop relative positioning algorithms for agricultural drone swarms in GPS-challenged environments. These algorithms should enable the determination of the relative positions of drones and the overall configuration of the swarm even in the complete absence of GPS signals, or with GPS signals available only to the operator. Algorithms should work even in case of long distances between drones.

3. Analysis of previous studies

This problem has been a persistent focus of scientific research, as evidenced by the large body of published research on the topic. We will now examine some of the most significant and pertinent studies.

Work [5] provides a taxonomy of drone positioning systems. The taxonomy categorizes drone positioning systems into two major methods: vision-based and non-vision-based. The taxonomy further divides each method into several sub-methods based on the equipment and calculation method. The taxonomy also provides the advantages and disadvantages of each method.

In the work [6] the effect of multiple sensors on 3D indoor position accuracy is investigated using the flexible Online Asynchronous State Estimation sensor fusion platform. However, this method is not suitable for agricultural drones, as they may operate over long distances from each other and in adverse weather conditions.

Work [4] explored the approach of replacing all the fixed anchors with a single drone that flies through a sequence of waypoints. At each waypoint, the drone acts as an anchor and securely determines the positions. However, this approach has proven a slow and ineffective solution.

Work [7] introduced several localization techniques that are independent of GPS, each with its advantages and disadvantages. Unfortunately, these disadvantages also make such techniques inapplicable for our case.

Work [8] offers the usage of a gray-scale low-resolution camera and an ultra-low-power System-on-Chip based on a novel vision, to use it with the fully convolutional neural network, however, for our task it faces the same disadvantages, as the approach, offered in [6].

In [9] topology perception and relative positioning algorithms were offered. But agricultural drones are mostly working at low altitudes over the fields – big similarly looking spaces – which makes this method inapplicable.

Our previous research [10] used granular computing and fuzzy sets but didn't provide accurate enough results to apply to the current task.

As we can see, existing solutions couldn't actually solve the problem, considering all its requirements and limitations. So, let's consider how it will be possible to determine the relative positions of drones and the overall configuration of the swarm even in the complete absence of GPS signals.

4. Main part

We begin the analysis of the proposed algorithm by describing the fundamental approach used – determining the direction and distance from each drone to every other drone. To determine the distance between a pair of drones, it is proposed to use either RSSI signal measurements [11] or the built-in distance measurement tools that are available on many models [12]. However, in any case, it is necessary to consider the presence of errors in signal measurement.

4.1. Application of radio modules for mutual positioning of drones

The primary purpose of classical radio modules is to complement the Internet of Things networks to enhance the capabilities of narrow artificial intelligence in sensor networks of smart homes, offices, and household devices equipped with radio beacons, such as electronic key fobs, smart vacuum cleaners, remote configuration of refrigerators and climate control equipment, etc. Such radio modules were developed to improve positioning accuracy in indoor environments, transmit sensor data over distances from a few centimeters to 300-600 meters, and interact with radio modules in smartphones and tablets. This approach effectively addresses challenges such as multipath reflections from walls, interference, and dead zones. By measuring the transmission time of a packet, radio module can achieve positioning accuracy within a margin of one centimeter.

Over the past eight years, numerous scientific studies and practical implementations have explored the use of such technologies for positioning small mobile robotic systems, such as wheeled robots and quadcopters. These systems can be organized into swarms, utilizing network-based technologies for coordinated operation [13], [14]. One of the tasks to be solved for controlling a swarm of drones [15] is to obtain an estimate of the coordinates of the swarm members in local and global coordinate systems [16].

The evaluation of local coordinates for a swarm element relative to others is achieved through direction-finding techniques, which rely on measuring the time of flight of a data packet transmitted between the swarm element and other network members (drones) and back. Radio modules equipped with omnidirectional antennas, characterized by a toroidal radiation pattern, are employed to calculate the distance between two drones within the swarm. Subsequently, a mathematical algorithm, potentially coupled with a calibration maneuver of the drone, is used to resolve any spatial uncertainty in positioning.

Adding a directional antenna to ready-made drone swarm radio modules is difficult, as it would require embedding into the highly integrated system-on-chip of the radio module. Some manufacturers provide the ability to connect a directional antenna, but the size and weight characteristics of such modules increase by 2-4 times.

4.2. Algorithm for calculating the distance from a drone to the position zone of another drone and the viewing angle from the drone to this zone

To accurately determine the directional angle of each drone relative to another, measuring only the distance between them is insufficient. Consequently, the deployment of two drones is required to measure the distance to a third drone, thereby facilitating the calculation of their respective angular positions. This concept will be elaborated upon in the following sections.

Figure 1 schematically depicts two drones, A and B, and a drone T (target), whose distance and angle must be determined.

Two circles are drawn centered at point A and two circles are centered at point B. These circles represent the distance from drones A and B to T plus or minus the measurement error. Due to the measurement error, T is not located at a specific point but rather in a certain zone formed by the intersection of these circles.

The distance between drones A and B is determined using the same methods as the distance to the drone T. Their relative positions can be refined using data acquired from cameras installed on these drones.

We are interested in the relationships between the various distances and angles shown in Figure 1. Let us illustrate these distances and angles in more detail in Figure 2.

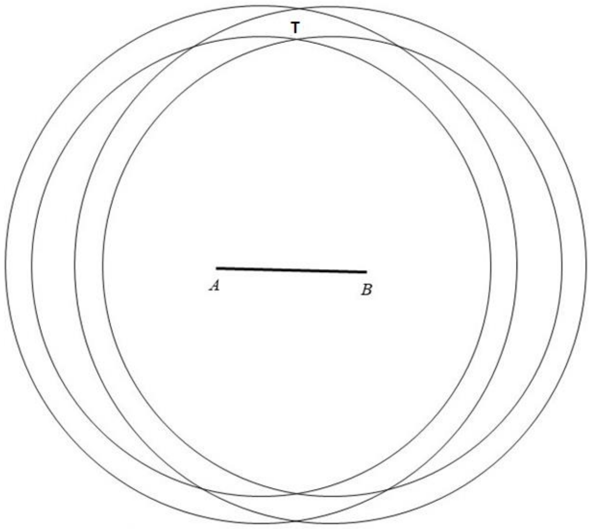

Figure 1: Schematic depiction of the calculated distances from two drones to a third

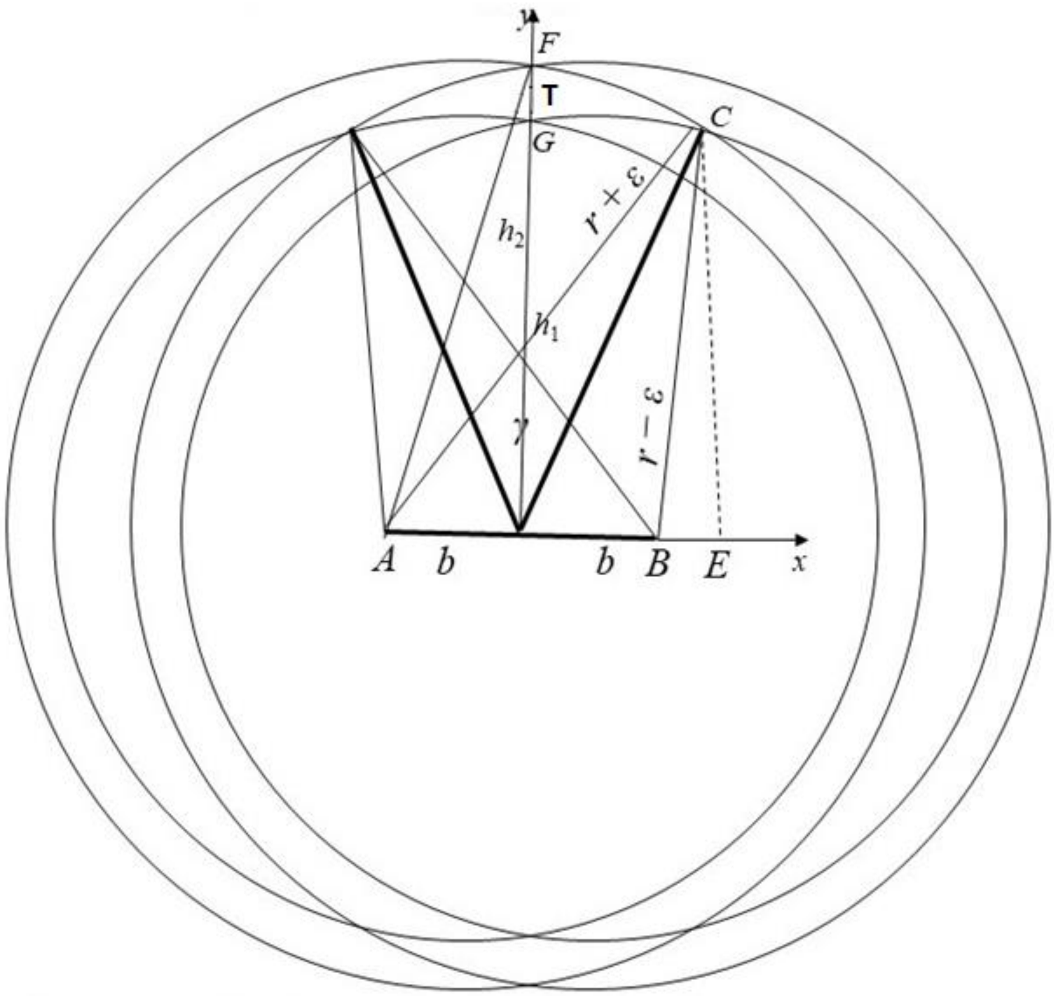

Figure 2: Distance and angle notation

We introduce a coordinate system and the following notation:

- x-axis is horizontal and aligned with the baseline AB
- y-axis is vertical and passes through the midpoint of AB to T
- AB – drones used for determining the position of a drone T
- r – measured distances from drones AB to T

- ε – the measurement errors of the distance r from drone to T
- b – half-length of the baseline – distance from the center of the segment AB to any end of this segment
- C – intersection point of the circle centered at point B with radius $r - \varepsilon$ and the circle centered at point A with radius $r + \varepsilon$
- G – point of intersection of two circles each having a radius of $r - \varepsilon$
- F – point of intersection of two circles each having a radius of $r + \varepsilon$
- E – orthogonal projection of point C onto the x-axis
- γ – angle of view from the midpoint of the AB segment at the T position locus
- h_1 – distance from the center of the segment AB to point G
- h_2 – distance from the center of the segment AB to point F

4.2.1. Relationship between *r, b* and *γ*

Firstly, we will show that the relationship between r, b and γ can be expressed by the following formulas:

$$tg\frac{\gamma}{2} = \frac{r\varepsilon}{\sqrt{(b^2-\varepsilon^2)(r^2-b^2)}} \tag{1}$$

$$r^2 = b^2\left[1 + \frac{\varepsilon^2}{(b^2-\varepsilon^2)tg^2\frac{\gamma}{2} - \varepsilon^2}\right] \tag{2}$$

For relatively large values of r, the term b can be neglected, and the formula (1) for the angle simplifies and becomes independent of r:

$$tg\frac{\gamma}{2} = \frac{r\varepsilon}{\sqrt{(b^2-\varepsilon^2)(r^2-b^2)}} \approx \frac{r\varepsilon}{\sqrt{(b^2-\varepsilon^2)r^2}} = \frac{\varepsilon}{\sqrt{b^2-\varepsilon^2}} \tag{3}$$

$$tg\frac{\gamma}{2} \approx \frac{\varepsilon}{\sqrt{b^2-\varepsilon^2}} \tag{4}$$

The formula (3) explains why calculations yield similar values for the angles for various large r.

The formula (4) also explains the similar values of b for large r and the independence of b from r.

$$tg\frac{\gamma}{2} \approx \frac{\varepsilon}{\sqrt{(b^2-\varepsilon^2)}} \Rightarrow b^2 \approx \frac{\varepsilon}{tg^2\frac{\gamma}{2}} + \varepsilon^2 \tag{5}$$

$$b^2 \approx \frac{\varepsilon^2}{tg^2\frac{\gamma}{2}} + \varepsilon^2 \tag{6}$$

4.2.2. Formulas for h_1 and h_2

$$h_1 = G_y = \sqrt{(r-\varepsilon)^2 - b^2} \tag{7}$$

$$h_2 = F_y = \sqrt{(r+\varepsilon)^2 - b^2} \tag{8}$$

When r in (7)-(8) is big enough: $h_2 - h_1 \approx 2\varepsilon$

Next, we will demonstrate how the presented relationships between parameters r, b and γ were obtained, and we will derive formulas for h_1 and h_2

4.2.3. Derivation of the relationship for *r, b* and *γ*

The x and y coordinates of point C.

Since C is the intersection point of the circle centered at B with radius $r-\varepsilon$ and the circle centered at A with radius $r+\varepsilon$, its coordinates can be found by solving the corresponding system of equations:

$$\begin{cases} B: (x-b)^2 + y^2 = (r-\varepsilon)^2 \\ A: (x+b)^2 + y^2 = (r+\varepsilon)^2 \end{cases} \Rightarrow \begin{cases} x^2 - 2xb + b^2 + y^2 = r^2 - 2r\varepsilon + \varepsilon^2 \\ x^2 + 2xb + b^2 + y^2 = r^2 + 2r\varepsilon + \varepsilon^2 \end{cases} \Rightarrow \tag{9}$$

Subtracting the first equation from the second in (9).

$$\Rightarrow 4xb = 4r\varepsilon \Rightarrow x = \frac{r\varepsilon}{b} \Rightarrow \tag{10}$$

Substituting x into equation B:$(x-b)^2+y^2=(r-\varepsilon)^2$, we can solve in (10) for y.

$$\Rightarrow y^2 = (r-\varepsilon)^2 - (x-b)^2 \Rightarrow y = \sqrt{(r-\varepsilon)^2 - (x-b)^2} \Rightarrow \sqrt{(r-\varepsilon)^2 - \left(\frac{r\varepsilon}{b} - b\right)^2}. \quad (11)$$

We chose the positive value of the root for y in (11) since point C is located above the horizontal axis.

Therefore,

$$C_x = \frac{r\varepsilon}{b}, C_y = \sqrt{(r-\varepsilon)^2 - (\frac{r\varepsilon}{b} - b)^2} \quad (12)$$

The viewing angle γ from AB center point to the target area T.

$$tg\frac{\gamma}{2} = \frac{C_x}{C_y} = \frac{r\varepsilon}{b\sqrt{(r-\varepsilon)^2 - (\frac{r\varepsilon}{b} - b)^2}} = \quad (13)$$

We will move b in (13) under the radical sign.

$$= \frac{r\varepsilon}{\sqrt{b^2(r-\varepsilon)^2 - (r\varepsilon - b^2)^2}} = \quad (14)$$

We will expand the brackets in (14) and collect like terms.

$$= \frac{r\varepsilon}{\sqrt{(r^2b^2 - 2r\varepsilon b^2 + \varepsilon^2 b^2) - (r^2\varepsilon^2 - 2r\varepsilon b^2 + b^4)}}$$

$$= \frac{r\varepsilon}{\sqrt{r^2b^2 + \varepsilon^2b^2 - \varepsilon^2b^2 - r^2\varepsilon^2 - b^4}} = \frac{r\varepsilon}{\sqrt{r^2b^2 - b^4 + \varepsilon^2b^2 - r^2\varepsilon^2}} \quad (15)$$

$$= \frac{r\varepsilon}{\sqrt{b^2(r^2 - b^2) - \varepsilon^2(r^2 - b^2)}} = \frac{r\varepsilon}{\sqrt{(b^2 - \varepsilon^2)(r^2 - b^2)}}$$

Therefore,

$$tg\frac{\gamma}{2} = \frac{r\varepsilon}{\sqrt{(b^2 - \varepsilon^2)(r^2 - b^2)}} \quad (16)$$

4.2.4. Measured distance between *A* and *T*

Let us solve equation (16) in terms of r.

$$tg\frac{\gamma}{2} = \frac{r\varepsilon}{\sqrt{(b^2 - \varepsilon^2)(r^2 - b^2)}} \Rightarrow (b^2 - \varepsilon^2)(r^2 - b^2)tg^2\frac{\gamma}{2} = r^2\varepsilon^2 \Rightarrow \quad (17)$$

Let us distribute the term outside the second parentheses in (17).

$$\Rightarrow (b^2 - \varepsilon^2)r^2tg^2\frac{\gamma}{2} - (b^2 - \varepsilon^2)b^2tg^2\frac{\gamma}{2} = r^2\varepsilon^2 \Rightarrow \quad (18)$$

Let's factor r^2 in (18).

$$\Rightarrow r^2\left[(b^2 - \varepsilon^2)tg^2\frac{\gamma}{2} - \varepsilon^2\right] = (b^2 - \varepsilon^2)b^2tg^2\frac{\gamma}{2} \Rightarrow \quad (19)$$

$$\Rightarrow r^2 = \frac{b^2(b^2 - \varepsilon^2)tg^2\frac{\gamma}{2}}{(b^2 - \varepsilon^2)tg^2\frac{\gamma}{2} - \varepsilon^2} \quad (20)$$

4.2.5. Measured *b* as half the base length – the distance between points *T* and *A*

Let us solve equation (17) in terms of b, as illustrated by

Figure **3**. We will square both sides of the equation.

$$tg\frac{\gamma}{2} = \frac{r\varepsilon}{\sqrt{(b^2 - \varepsilon^2)(r^2 - b^2)}} \Rightarrow tg^2\frac{\gamma}{2} = \frac{r^2\varepsilon^2}{(b^2 - \varepsilon^2)(r^2 - b^2)} \Rightarrow \quad (21)$$

Let us expand the parentheses in (21).

$$\Rightarrow tg^2\frac{\gamma}{2} = \frac{r^2\varepsilon^2}{r^2b^2 + \varepsilon^2b^2 - r^2\varepsilon^2 - b^4} \Rightarrow \quad (22)$$

$$\Rightarrow tg^2\frac{\gamma}{2}(r^2b^2 + \varepsilon^2b^2 - r^2\varepsilon^2 - b^4) = r^2\varepsilon^2 \quad (23)$$

By collecting at (23) the coefficients of b^2 and b^4, we obtain a quadratic equation in b^2.

$$(b^2)^2 - (r^2 + \varepsilon^2)b^2 + r^2\varepsilon^2(1 + \frac{1}{tg^2\frac{\gamma}{2}}) = 0 \Rightarrow \tag{24}$$

$$b^2 = \frac{r^2 + \varepsilon^2 \pm \sqrt{(r^2 + \varepsilon^2)^2 - 4r^2\varepsilon^2(1 + \frac{1}{tg^2\frac{\gamma}{2}})}}{2} \Rightarrow \tag{25}$$

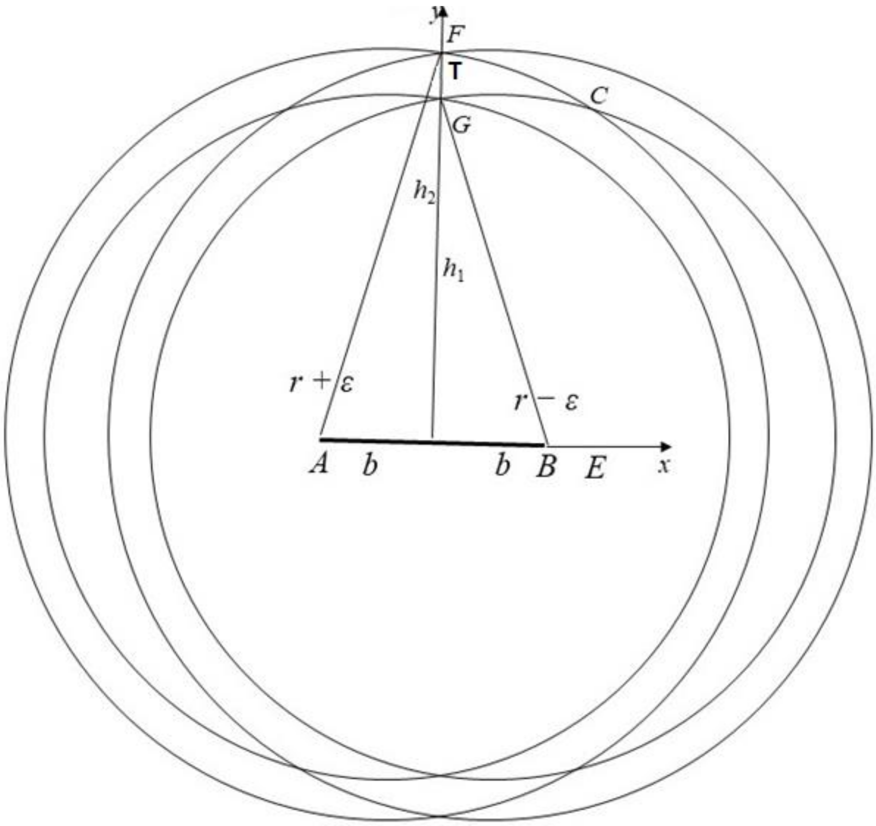

Figure 3: Illustration of the derivation of formulas for h_1 and h_2

We will express in (25) tangent as sine over cosine.

$$b^2 = \frac{r^2 + \varepsilon^2 \pm \sqrt{(r^2 + \varepsilon^2)^2 - 4r^2\varepsilon^2(1 + \frac{cos^2\frac{\gamma}{2}}{sin^2\frac{\gamma}{2}})}}{2} \Rightarrow \tag{26}$$

$$b^2 = \frac{r^2 + \varepsilon^2 \pm \sqrt{(r^2 + \varepsilon^2)^2 - 4r^2\varepsilon^2(\frac{sin^2\frac{\gamma}{2} + cos^2\frac{\gamma}{2}}{sin^2\frac{\gamma}{2}})}}{2} \Rightarrow \tag{27}$$

$$b^2 = \frac{r^2 + \varepsilon^2 \pm \sqrt{(r^2 + \varepsilon^2)^2 - \frac{4r^2\varepsilon^2}{sin^2\frac{\gamma}{2}}}}{2} \tag{28}$$

We take only the negative sign in front of the radical to ensure that $b^2 > 0$.

$$b^2 = \frac{r^2 + \varepsilon^2 - \sqrt{(r^2 + \varepsilon^2)^2 - 4r^2\varepsilon^2(\frac{sin^2\frac{\gamma}{2} + cos^2\frac{\gamma}{2}}{sin^2\frac{\gamma}{2}})}}{2} \Rightarrow \tag{29}$$

4.2.6. Derivation of formulas for h_1 and h_2

Given that G is the intersection point of two circles with radius $r–\varepsilon$ and F is the intersection point of two circles with radius $r+\varepsilon$, from

Figure **3** and the Pythagorean theorem.

$$h_1 = G_y = \sqrt{(r-\varepsilon)^2 - b^2} \tag{30}$$

$$h_2 = GA_y = \sqrt{(r+\varepsilon)^2 - b^2} \tag{31}$$

When r in (30)-(31) are big:

$$h_1 = \sqrt{(r-\varepsilon)^2 - b^2} \approx \sqrt{(r-\varepsilon)^2} = r - \varepsilon \tag{32}$$

$$h_2 = \sqrt{(r+\varepsilon)^2 - b^2} \approx r+\varepsilon \tag{33}$$

Therefore,

$$h_2 - h_1 \approx 2\varepsilon \tag{34}$$

So, we can determine the relative positions of the swarm elements with high precision.

4.3. The Problem of Poor Angles Between Drones

The schemes for determining the relative positions of drones in a swarm, considered in the previous sections, are well-suited for the case of a successful relative arrangement of three drones used to determine each other's position (Figure 4).

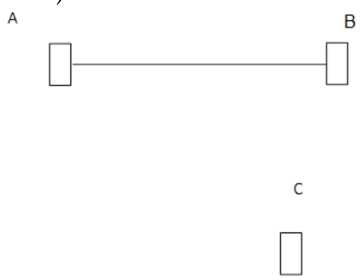

Figure 4: An example of good relative positioning of drones for determining their mutual position

However, other scenarios are possible, including the worst-case scenario where all three drones are located in the same straight line (Figure 5**Figure 5**). The problem of acute or obtuse angles can be solved by hardware means by rotating one or two drones temporarily by 90 degrees if the algorithm described in the previous sections detects that the current angle between the drones produces large measurement errors.

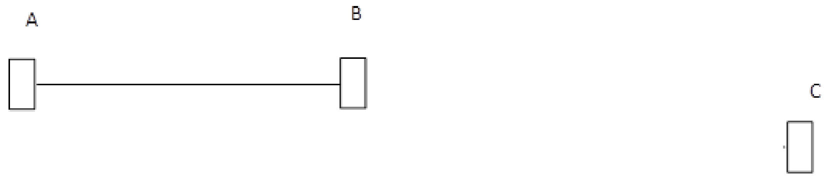

Figure 5: An example of poor relative positioning of drones for determining their mutual position

Options for adjusting sensor positions. The conditions for improving direction finding in a drone can be created by rotating one drone relative to another (Figure 6).

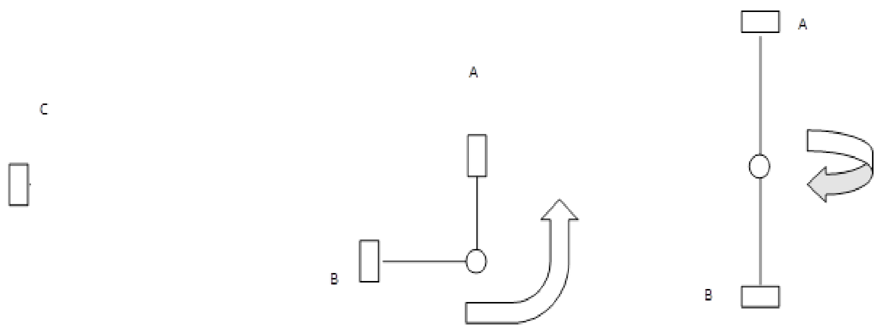

Figure 6: Possible approaches to enhance the accuracy of determining a drone's direction

4.4. Practical Testing

The derived formulas were validated experimentally by creating several test datasets for various relative positions of three drones and different distances between them. The obtained results confirmed the operability of the created mathematical model, allowing the determination of the relative position of drones in a swarm relative to each other (Figure 7).

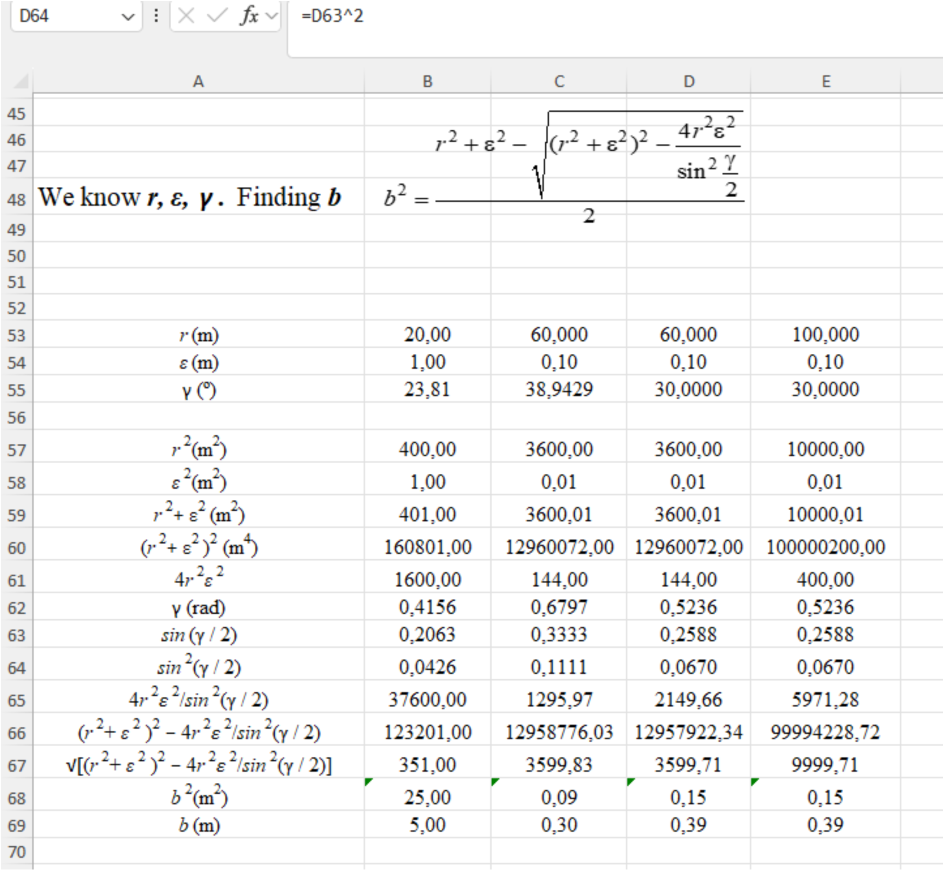

D64 =D63^2

We know ***r, ε, γ***. Finding ***b***

$$b^2 = \frac{r^2 + \varepsilon^2 - \sqrt{(r^2+\varepsilon^2)^2 - \dfrac{4r^2\varepsilon^2}{\sin^2\frac{\gamma}{2}}}}{2}$$

	B	C	D	E
r (m)	20,00	60,000	60,000	100,000
ε (m)	1,00	0,10	0,10	0,10
γ (°)	23,81	38,9429	30,0000	30,0000
r^2(m^2)	400,00	3600,00	3600,00	10000,00
ε^2(m^2)	1,00	0,01	0,01	0,01
$r^2+\varepsilon^2$ (m^2)	401,00	3600,01	3600,01	10000,01
$(r^2+\varepsilon^2)^2$ (m^4)	160801,00	12960072,00	12960072,00	100000200,00
$4r^2\varepsilon^2$	1600,00	144,00	144,00	400,00
γ (rad)	0,4156	0,6797	0,5236	0,5236
sin (γ / 2)	0,2063	0,3333	0,2588	0,2588
sin^2(γ / 2)	0,0426	0,1111	0,0670	0,0670
$4r^2\varepsilon^2/sin^2(\gamma/2)$	37600,00	1295,97	2149,66	5971,28
$(r^2+\varepsilon^2)^2 - 4r^2\varepsilon^2/sin^2(\gamma/2)$	123201,00	12958776,03	12957922,34	99994228,72
$\sqrt{[(r^2+\varepsilon^2)^2 - 4r^2\varepsilon^2/sin^2(\gamma/2)]}$	351,00	3599,83	3599,71	9999,71
b^2(m^2)	25,00	0,09	0,15	0,15
b (m)	5,00	0,30	0,39	0,39

Figure 7: An example of the practical validation of the derived formulas for determining the relative position of swarm elements

5. Conclusions

Autonomous swarm elements enable precise, large-scale monitoring and management of agricultural tasks, optimizing resource use and reducing labor requirements. As a result of this study, the algorithm for determining the relative position of swarm elements in the absence of GPS signals and the corresponding mathematical apparatus was developed. It takes into account possible inaccuracy of distance measurement.

Various configurations of potential relative positions within swarm elements, their influence on the accuracy of relative position determination, and solutions to issues arising from suboptimal initial configurations were analyzed. The results were validated through practical computational models. The obtained results confirmed the operability of the created mathematical model, giving measurement error of 1 percent or less.

Future research will focus on the practical application and empirical evaluation of these findings within operational drone swarms. Special attention will be directed towards enhancing the relative positioning accuracy of closely spaced drones using visual techniques, particularly by integrating advanced computer vision algorithms.

Declaration on Generative AI

The authors have not employed any Generative AI tools.

References

[1] M. R. Dileep, A. V. Navaneeth, et al. A study and analysis on various types of agricultural drones and its applications, in: Proc. of the 2020 fifth Intern. Conf. on research in computational intelligence and comm. networks, IEEE, 2020, pp. 181–185. doi:10.1109/ICRCICN50933.2020.9296195

[2] D. Albani, J. Ijsselmuiden, et al. Monitoring and mapping with robot swarms for agricultural applications, in: Proceedings of the 2017 14th IEEE International Conference on Advanced Video and Signal Based Surveillance, IEEE, 2017, pp. 1-6. doi:10.1109/AVSS.2017.8078478

[3] S. Carberry, Base Defense: Evolving Threats Require New Approaches to Defending Installations, National Defense, 107(834), 2023, pp. 22-24. URL: https://www.nationaldefensemagazine.org/articles/2023/4/21/evolving-threats-require-new-approaches-to-defending-installations

[4] P. Perazzo, F. B. Sorbelli, et al.. Drone path planning for secure positioning and secure position verification. IEEE Trans. on Mobile Comp. 16, no. 9 (2016): 2478-2493. doi:10.1109/TMC.2016.2627552

[5] F. Jametoni and D. E. Saputra, A Study on Autonomous Drone Positioning Method, in: Proceedings of the 2021 6 Intern. Conf. on Informatics and Computing (ICIC), IEEE, 2021, pp. 1-5. doi:10.1109/ICIC54025.2021.9632926

[6] J. Gerwen, K. Geebelen, et al. Indoor drone positioning: Accuracy and cost trade-off for sensor fusion. IEEE Transactions on Vehicular Technology, Vol. 71, no. 1 (2021): 961-974. doi:10.1109/TVT.2021.3129917

[7] J.-H.Kang, K.-J. Park, et al., Analysis of localization for drone-fleet, in: Proc. of the 2015 Intern. Conf. on Inform. and Comm. Techn. Convergence (ICTC), IEEE, 2015, pp. 533-538. doi:10.1109/ICTC.2015.7354604

[8] L. Crupi, A. Giusti, et al. High-throughput visual nano-drone to nano-drone relative localization using onboard fully convolutional networks. arXiv preprint arXiv:2402.13756 (2024).

[9] Di, Chengliang, and Xiaozhou Guo. Topology Perception and Relative Positioning of UAV Swarm Formation Based on Low-Rank Optimization. Aerospace 11, no. 6 (2024): 466. doi:10.3390/aerospace11060466

[10] M. Ogurtsov, V. Korolyov, O. Khodzinskyi, Improving the Productivity of UAV Operations Based on Granular Computing and Fuzzy Sets, in: Proc. of the 2021 IEEE 6th Intern. Conf. on Actual Problems of Unmanned Aerial Vehicles Development (APUAVD) 19-21 Oct. 2021, 2021, pp. 33-36. doi:10.1109/APUAVD53804.2021.9615419.

[11] A. Aksoy, Ö. Yıldız, and S. E. Karlık. Comparative Analysis of End Device and Field Test Device Measurements for RSSI, SNR and SF Performance Parameters in an Indoor LoRaWAN Network. Wireless Personal Comm. 134, no. 1 (2024): 339-360. doi:10.1007/s11277-024-10911-z

[12] M. Džunda, P. Dzurovčin, S. Čikovský, and L. Melníková. "Determining the Location of the UAV When Flying in a Group." Aerospace 11, no. 4 (2024): 312. doi:10.3390/aerospace11040312

[13] J Lee, C. Y, Cooperative drone positioning measuring in internet-of-drones, in: 2020 IEEE 17th Ann. Consumer Comm. & Networking Conference (CCNC), IEEE, 2020, pp. 1-3.

[14] P. V. Klaine, J. P. Nadas, R. D. et al.. Distributed drone base station positioning for emergency cellular networks using reinforcement learning. Cogn. computation, 10(5) (2018): 790-804.

[15] Wu Chen, Jiayi Zhu, et al. A fast coordination approach for large-scale drone swarm. Journal of Network and Computer Applications 221 (2024): 103769.

[16] Yu. Wang, He Li, Zechen Tang et al.. "DeepH-2: Enhancing deep-learning electronic structure via an equivariant local-coordinate transformer." arXiv preprint arXiv:2401.17015 (2024).